CHAPTER SIX

Spatial Models of Soil Erosion and GIS

JOHN P. WILSON AND MARK S. LORANG

6.1 INTRODUCTION

Numerous soil erosion models have been developed during the past fifty years to estimate rates of soil erosion under different land use systems. By 1970, the Universal Soil Loss Equation (USLE) had emerged as the leading model (Meyer, 1984) and it has been widely used by the staff of the Natural Resource Conservation Service (NRCS) of the US Department of Agriculture to help define acceptable agricultural practices on highly erodible land during the past three decades (Foster, 1991). The USLE was recently updated and the Revised Universal Soil Loss Equation (RUSLE) has now been substituted in place of the original model for farm conservation planning in the USA (Glanz, 1994; Kautza *et al.*, 1995). RUSLE, in turn, will be replaced by the Water Erosion Prediction Project (WEPP) model during the next decade (Laflen *et al.*, 1997).

The USLE and RUSLE are statistical models that were designed to predict soil erosion on individual slope profiles. However, the widespread occurrence and importance of accelerated soil erosion and related water quality problems (Pimental *et al.*, 1995) have generated a need for soil erosion assessments at scales ranging from individual farm fields to large catchments and various types of administrative units (counties, provinces, states, and so on). In addition, the advent of GIS has promoted an explosive growth in the number and variety of GIS-based model applications at catchment and larger scales during the past decade (see, for example, Gilliland and Baxter-Potter, 1987; Hession and Shanholtz, 1988; Sivertun *et al.*, 1988; Ventura *et al.*, 1988; Warren *et al.*, 1989; Huang and Ferng, 1990; Flache *et al.*, 1990; James and Hewitt, 1992; Tim *et al.*, 1992). However, the GIS technology and soil erosion models were developed by different groups of scientists with different disciplinary backgrounds and traditions, and the potential benefits and limitations of this integration warrant closer scrutiny (Moore *et al.*, 1992, 1993b).

This chapter has four objectives. First, the methods with which data are compiled and analyzed in traditional applications of the USLE and RUSLE models are

reviewed. Second, the ways in which GIS can be used to obtain USLE/RUSLE model inputs more quickly and easily are identified. Third, the paths by which the inappropriate use of GIS may lead to questionable USLE/RUSLE model results are explored. Fourth, some of the ways in which GIS is being used to develop improved models for performing soil erosion assessments at catchment and larger scales are examined.

6.2 TRADITIONAL APPLICATIONS OF THE USLE AND RUSLE MODELS

The USLE is a simple multiplicative model that was empirically derived from over 10 000 plot-years of data (Wischmeier and Smith, 1965, 1978). It can be written as:

$$A = R\,K\,C\,P\,L\,S \tag{6.1}$$

where A is the mean soil loss in tonnes per hectare over the entire slope length, R is the rainfall-runoff erosivity factor, K is a soil erodibility factor, C is a cover management factor, P is a supporting practices factor, L is a slope length factor and S is a slope steepness factor. R is the product of the storm total kinetic energy and the maximum 30 minute intensity for qualifying storms. K is expressed as soil loss per unit of R for a unit plot. The standard USLE unit plot was 22.13 meter long with a uniform width and uniform 9 percent slope maintained in continuous fallow, with tillage when necessary to break up surface crusts. C is a dimensionless factor representing the ratio of soil loss from the condition of interest to that from a tilled continuous fallow. P is a dimensionless factor representing the ratio of soil loss with practices such as contouring, stripcropping or terracing, to that with farming up-and-down the slope. L is a dimensionless factor representing the ratio of soil loss from a given slope length to that from a 22.13 meter slope length under the same conditions. S is a dimensionless factor representing the ratio of soil loss from a given slope steepness to that from a 9 percent slope under the same conditions (Meyer, 1984).

The model is used to compare soil erosion from individual farm fields to that expected from a 'standard' soil-loss plot. The USLE defines soil loss as the amount of eroded soil and how far it has moved downslope (Yoder and Lown, 1995). The model predicts detachment-limited erosion on planar hillslopes and it is not applicable to areas experiencing net deposition (Foster and Wischmeier, 1974; Griffin *et al.*, 1988; Foster, 1991). Hence, the predicted soil loss is not equal to the delivery of sediment to the bottom of the slope if deposition occurs on the slope and the USLE should not be applied to areas experiencing net deposition (Wischmeier, 1976; Wilson, 1986; Foster, 1991). The delivery of sediment to the bottom of the slope is often the parameter of interest in water quality models. Similarly, the model was designed to predict long-term average annual erosion rates and it may not perform very well if it is applied to single storms and/or single calendar years (Wischmeier, 1976; Yoder and Lown, 1995).

The model inputs are usually estimated from maps and/or field measurements. Rainfall-runoff erosivity is represented by R and can be computed directly from rainfall intensities and amounts. Maps of R are available for the conterminous USA and they show how R varies on a regional scale. Soil erodibility is represented by K, and in the USA values of K have been measured or interpolated (from soil texture, organic matter content and permeability data) for all mapped soil series as part of the county soil survey program. Soil series are mapped at scales of 1:15 000 to 1:20 000 in these surveys. Land use and management are represented by C and P and can be estimated

from field reconnaissance and/or farm records (Wilson and Ryan, 1988; Wilson, 1989; Busacca *et al.*, 1993). C and P may also, with some difficulty, be inferred from aerial photography or remotely sensed imagery combined with ground-truth data (Morgan *et al.*, 1978, 1979, 1980; Stephens *et al.*, 1985).

The effects of topography on soil loss are characterized by the combined LS factor. Representative slope gradients and slope lengths were usually measured manually in the field or from topographic maps and plugged into the following equation:

$$LS = \left(\frac{\lambda}{22.13}\right)^{m} [65.4 (\sin \beta)^2 + 4.56 \sin \beta + 0.0654] \tag{6.2}$$

where L and S are the slope length and slope steepness factors from equation (6.1), λ is the slope length in meters, m is a constant dependent on the value of slope gradient, and β is the slope gradient in degrees (Wischmeier and Smith, 1965, 1978). This equation predicts increased erosion for long, steep, planar hillslopes with negligible convergence/divergence. Foster and Wischmeier (1974) later divided irregular slopes into a series of uniform segments (Figure 6.1) and modified the original LS equations to calculate the average soil loss along these irregular hillslope profiles:

$$LS = \frac{\sum_{i=1}^{n} (\lambda_i^{m+1} - \lambda_{i-1}^{m+1})\, S_i}{\lambda_c (22.13)^m} \tag{6.3}$$

where S_i is the slope steepness factor for the ith segment, λ_i is the length from the top of the slope to the lower end of the ith segment, λ_{i-1} is the length from the top of the slope to the upper end of the ith segment, λ_c is the overall slope length, n is the number of uniform segments, and m is the slope length exponent (as in equation 6.2). A variant of equation 6.3 can be used to estimate the effective LS factor value for the ith segment as follows:

$$LS_i = \frac{(\lambda_i^{m+1} - \lambda_{i-1}^{m+1})\, S_i}{(\lambda_i - \lambda_{i-1})\, 22.13^m} \tag{6.4}$$

Notwithstanding these innovations, estimation of the LS factor has posed more problems than any of the other factors in the USLE (Wilson, 1986; Renard *et al.*, 1991; Moore and Wilson, 1992, 1994). The delineation of the bottoms of qualifying slopes and the division of irregular slopes into a series of uniform segments (similar to Figure 6.1) can have a large impact on computed LS factor values. These problems, as we will see shortly, also occur when extending the application of the model from slope profiles to catchments and larger regions.

RUSLE retained the basic structure of the original model but incorporated new factor values that were based on the analysis of thousands of new erosion measurements (Renard *et al.*, 1991, 1993, 1994). The latest versions (2.0 and higher) also provide users with a Windows interface (Yoder and Lown, 1995). The major modifications are:

1. The inclusion of revised R factor values for the western USA based on data for more climate stations and a correction to R to reflect the effect of raindrop impact for flat slopes striking water ponded on the surface.
2. The ability to adjust K factor values to account for seasonal changes such as freezing and thawing, soil moisture and soil consolidation.

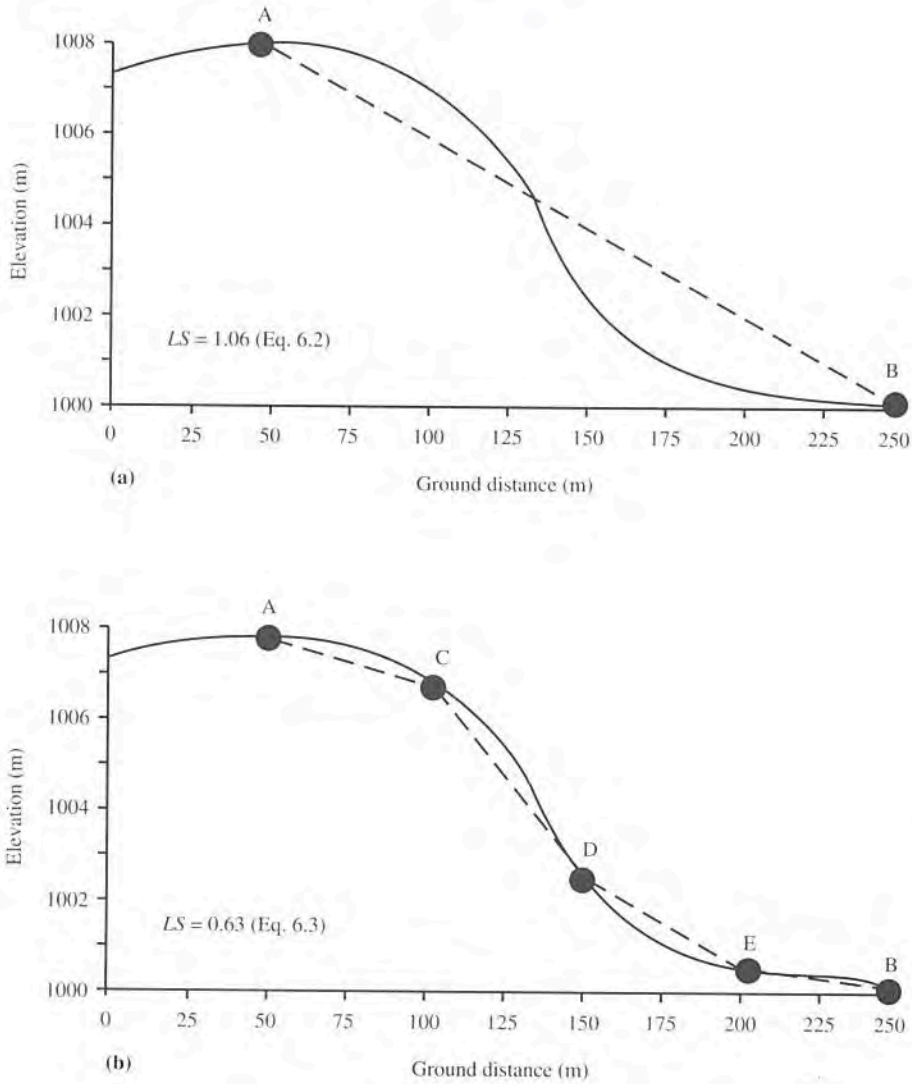

Figure 6.1 Schematic diagrams showing typical USLE slope profiles for (a) uniform and (b) irregular slopes. Solid circles delineate line segments.

3 The inclusion of a series of subfactors representing prior land use, canopy cover, surface cover, surface roughness and soil moisture in place of lumped factor values based on crop and tillage conditions for calculating C factor values.

4 The ability to modify soil loss estimates in response to tillage operations, changes in residue conditions, etc. as they occur throughout the year.

5 The development of a series of new and improved empirical equations for estimating the LS factor:

$$LS = \left(\frac{\lambda}{22.13}\right)^{m} (10.8 \sin \beta + 0.03) \qquad \text{when } \sin \beta < 0.0896 \tag{6.5a}$$

$$LS = \left(\frac{\lambda}{22.13}\right)^{m} (16.8 \sin \beta - 0.5) \qquad \text{when } \sin \beta \geq 0.0896 \tag{6.5b}$$

where λ is the slope length in meters, β is the slope in degrees, and $m = F/(1 + F)$, with $F = (\sin \beta/0.0896)/[(3\sin \beta)^{0.6} + 0.56]$ or $F = 0$ when there is deposition (McCool *et al.*, 1987, 1989; Renard *et al.*, 1994). This pair of equations also predicts increases in erosion with increases in slope gradient and slope length on planar hillslopes, and they ignore the influence of flow convergence/divergence (i.e. assume slopes of uniform width similar to the earlier equations).

Several attempts were made to apply the USLE to catchments prior to the advent of GIS (Williams and Berndt, 1972, 1977; Morgan and Nalepa, 1982; Wilson, 1986, 1989; Griffin *et al.*, 1988; Wilson and Ryan, 1988). In one such study, Wilson (1989) used a random, systematic sampling design to choose slope profiles for a series of catchments in the Lake Simcoe–Couchiching Basin, Ontario, Canada, and calculated length-slope factor distributions for each catchment. The profiles were divided into uniform slope segments, and a series of logical rules based on landscape position and profile curvature were used to identify slope segments likely to experience net deposition (Wilson, 1986). Length-slope factors were calculated using the methodology of Foster and Wischmeier (1974) and combined with the other factors to estimate catchment soil losses using a complicated series of rules based on qualitative descriptions of topography and crop productivity in published county soil surveys (Wilson, 1989). The exact locations of the slope profiles did not matter in this application because (1) the locations of cover management types were not known (Wilson and Ryan, 1988), and (2) the objective was to estimate average annual long-term watershed sediment and phosphorus loadings to Lake Simcoe. This catchment study honored the slope gradient and slope gradient definitions in the original USLE, but at the cost of not being able to predict erosion at specific locations in the landscape.

Griffin *et al.* (1988) compared various manual methods for computing the length-slope factor and rewrote the original USLE to calculate erosion at any point in the landscape as follows:

$$A = (m + 1)\, R\, K\, C\, P\, (\lambda_p/22.13)^{m} S \tag{6.6}$$

where λ_p is the slope length from the drainage divide to the point of interest in the landscape and m is the slope length exponent. This version of the USLE adds a new scalar $(m + 1)$ and a modified slope length term λ_p so that erosion can be estimated at specific locations in catchments without first dividing them into USLE slope profiles. We will see later that this version is similar to equation 6.4 but is much easier to implement in a GIS than the original equation because it uses a raster data structure. However, the user must still find a way to distinguish those areas experiencing net erosion and deposition prior to using the equation. This last task represents a major practical problem because the model itself does not distinguish those parts of hillslope profiles experiencing net erosion and net deposition.

The results from a recent study in a 46 hectare closed catchment in the Palouse region of northern Idaho illustrate the challenges and difficulties involved in extending the application of the model from individual slope profiles to farm fields and larger spatial units. Busacca *et al.* (1993) used cesium-137 to measure net soil loss or gain at 143 sampling points. Cesium-137, a radioisotope by-product of atmospheric nuclear weapons testing programs, has been successfully used to document patterns of

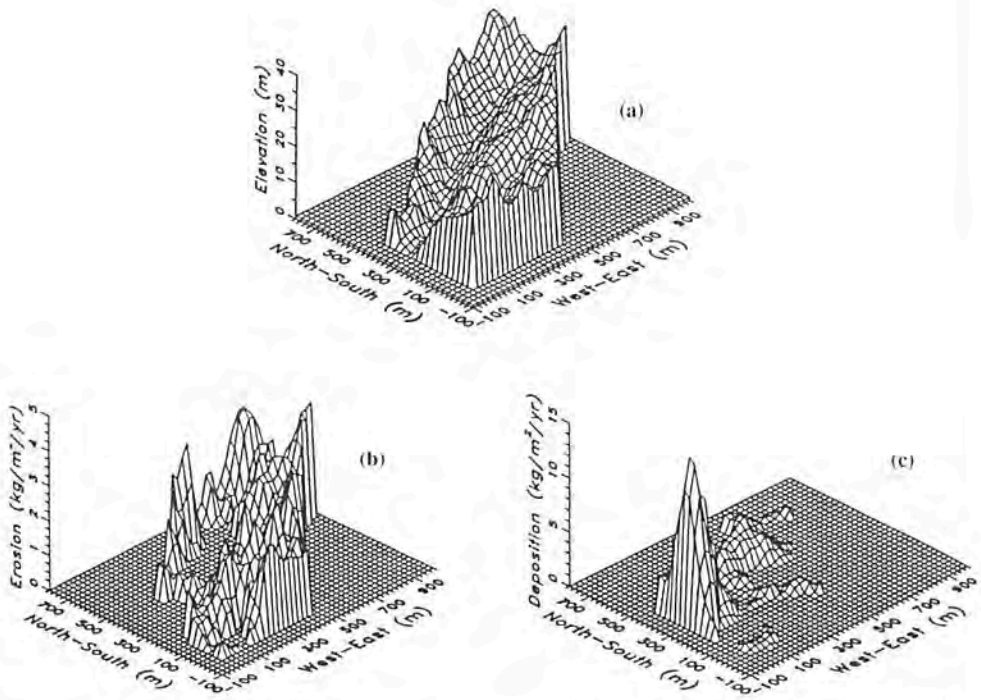

Figure 6.2 Three-dimensional maps showing (a) relative elevation of Palouse study site (15 × vertical exaggeration), (b) kriged soil deposition rates, and (c) kriged soil erosion rates across study watershed. (After Busacca *et al.*, 1993, pp. 365–366.)

erosion and deposition in fields (Ritchie and McHenry, 1990). Net erosion averaged 11.6 tonnes per hectare per annum from erosional areas in the watershed (about 60 percent of the study area, see Figure 6.2b) and deposition averaged 18.6 tonnes per hectare per annum onto depositional areas of the watershed (40 percent of study area, see Figure 6.2c). RUSLE was applied to the same field as follows. A single R factor value of 65 that accounted for the seasonal effects of thawing soil and rain falling on snow or partly frozen soil was used. An average K factor value of 0.32 was calculated from NRCS records. Single C and P factor values of 0.95 and 0.23, respectively, were estimated by the authors after interviewing current and former farm operators and examining written management records extending back to the 1930s. A single LS factor value of 3.10 was estimated by calculating LS for several 'representative' transects and taking a simple average. The average erosion rate estimated by RUSLE for the entire watershed of 31.4 tonnes per hectare per annum was nearly three times the average rate estimated by kriged cesium-137 data of 11.6 tonnes per hectare per annum for erosional areas.

These results illustrate the importance of identifying net deposition zones before application of the model and some of the deficiencies with the input data (as noted by the authors) and/or the RUSLE model itself. The cesium-137 results, for example, incorporated the effects of tillage erosion in addition to the detachment-limited erosion processes envisaged in RUSLE. This state of affairs coupled with the simple averaging of K and LS factor values and their choice of 'representative' transects for the LS factor calculations might help to explain the discrepancies between the

cesium-137 and RUSLE soil erosion estimates. Several of these problems can be traced to the ways in which the landscape was delineated into map units and how the attributes (model inputs) were aggregated (estimated) in each map unit. We will see shortly that these concerns about the methods and/or types of spatial organization (data structures, resolution and so on) used to estimate USLE factor values also have important implications for GIS-based soil erosion model applications.

6.3 IMPLEMENTING SOIL EROSION MODELS WITH GIS

The applications that have combined GIS with soil erosion models have attempted to exploit one or other of two potential advantages. One is the potential use of GIS to estimate and combine existing model inputs more accurately, and the other is the potential of using GIS to develop new or improved models. These possibilities are examined in turn below.

6.3.1 GIS-based applications of USLE and RUSLE

The primary role of the GIS in USLE and RULSE applications has been to generate, store and display model inputs and outputs. However, these applications have varied in terms of the type and intensity of coupling (as defined by Nyerges, 1992) used to link the GIS of choice and USLE, and the methods used to generate and organize the spatially distributed model inputs. The applications described below illustrate three of the approaches that have been tried and some of the advantages and disadvantages that follow from coupling these models with GIS software and/or data.

Hession and Shanholtz (1988) combined the Map Analysis Package (MAP) developed by Tomlin (1980) with the USLE and a sediment delivery ratio to estimate potential sediment loadings to streams from agricultural land in Virginia's Chesapeake Bay. A single R was obtained from published maps and used for each county. K was obtained from county soil survey reports. LS was calculated for each cell by inserting slope length and the average cell slope into the appropriate USLE equations. C was determined from Landsat imagery, and P was assumed to be constant and equal to unity. Cell slopes were determined by weighting the slope between each cell and its eight neighbors. All data, with the exception of elevation, were encoded for 1 hectare (100×100 m) grid cells. Elevation data were sampled at a 4 hectare cell resolution (200 m by 200 m) and 1 hectare maps were generated with computer software because of cost constraints. The majority rule was used to assign cell values for discontinuous data such as soil type, and the centroid value was assigned to each cell for continuous data such as elevation. A delivery ratio was then calculated for each agricultural land cell and combined with the USLE soil erosion value to estimate the sediment that reaches a stream.

Ventura *et al.* (1988) used a series of GIS polygon overlays and Fortran programs to estimate soil erosion in Dane County, Wisconsin. A seamless digital soil map of the entire county was prepared from 181 detailed soil maps and used to assign R, K and LS factor values. Five land cover types were classified from a Landsat TM scene acquired in August 1984 and converted to a polygon coverage that was compatible with the other GIS data. A composite land-cover layer consisting of Public Land Survey System (PLSS) quarter sections, incorporated areas, wetlands and satellite land cover

(five classes) was then created and combined with the soils layer via a polygon-on-polygon topological overlay. The USLE was used to estimate soil erosion for the 500 000 polygons (0.4 ha average size) labeled as row crop and hay/meadow areas.

The third project by James and Hewitt (1992) used a series of ARC/INFO coverages and Arc Marco Language (AML) programs to build a decision support system for the Blackfoot River drainage in Montana. This decision support system was based on the Water Resources Evaluation of Nonpoint Silvicultural Sources (WRENSS) model that, in turn, incorporates a modified version of the USLE to estimate potential soil erosion. *R* was estimated from published isoerodent maps and historic snow survey data. *K* values were estimated from a series of digital and paper NRCS and Forest Service soil surveys. *LS* values were estimated from 1:250 000 scale digital elevation models (DEM) with the GRID tools in ARC/INFO. A land-cover data layer was prepared from a Landsat TM scene. Some additional data processing was necessary because (1) some of the soil survey source maps delineated soil mapping units and others delineated Forest Service land-type units at scales ranging from 1:250 000 to 1:24 000, (2) the topographic factor estimates had to be resampled to a larger cell size, stratified into classes, and converted to a vector format to ensure compatibility with the other model data layers, and (3) a generalized land-cover data layer was generated without the benefit of extensive ground-truth data. The user interface developed as part of this decision support system is geared towards data browsing and querying at the basin level and data modeling at the subwatershed level. Hence users are able to estimate soil erosion rates under a variety of land-cover conditions for a series of third-order watersheds.

These applications illustrate two sets of advantages that can accrue from implementing these models with GIS. Part of the value of using GIS can be ascribed to the coordinate registration and overlay functions that are common to most GIS. These functions have provided new opportunities to organize and combine data based on geographic location and they allow these types of model to be applied to larger regions at finer resolutions. All three of the GIS-based applications described above demonstrate this benefit, although Hession and Shanholtz (1988) used a raster-based GIS and transformed the USLE into a raster-based model, whereas the other applications used the polygon data structure of a vector-based GIS and transformed the USLE into a polygon-based model. The remainder of the benefit is acquired from using one or more GIS functions to estimate USLE/RUSLE factor values. The magnitude of this benefit varies by model input. The three sample applications described above used existing maps of rainfall-runoff erosivity (*R*) and soil erodibility (*K*) and ignored the supporting practices (*P*) factor altogether. Hence, no additional value was added with the GIS in these instances. However, they all used GIS and/or remote sensing software to predict crop management (*C*) factor values, and two of the three applications used GIS to generate topographic (*LS*) factor values. A closer examination of these components indicates that some additional value was added by using the GIS in these instances.

All three of these applications exploited the tremendous potential of Landsat TM imagery to provide spatially distributed estimates of land cover. Earth-observing satellites, such as Landsat and SPOT, have been collecting data for more than twenty years (Loveland *et al.*, 1995). These data are routinely used for land-cover assessment, although several practical problems have limited their usefulness for estimating the cropping management factor (as discussed below). In addition, the large volumes of data and the complexity of data acquisition and analysis make this approach

prohibitively expensive for all but small areas (Woodwell *et al.*, 1984). Recent attempts to prepare land-cover assessments for large areas (multiple counties, states, continents) have focused on the potential application of meteorological satellite data for such ventures (Loveland *et al.*, 1995). The multilevel, digital, geographically referenced land-cover database prepared from multidate, meteorological satellite imagery acquired by the National Oceanic and Atmospheric Administration's (NOAA) Advanced Very High Resolution Radiometer (AVHRR) sensor complemented by ancillary spatial data for the conterminous US by Loveland *et al.* (1995) illustrates this potential. Their maps identified 159 distinct land-cover classes at a spatial resolution of 1 km^2.

However, there are at least two further challenges with this approach. First, the acquisition of the additional information about prior land use, canopy and surface cover, surface roughness and soil moisture needed to transform land-cover types into *C* factor values is fraught with difficulties. Satellite imagery cannot provide these inputs and one must revert to time-consuming methods or generalized estimates. Wilson and Ryan (1988) calculated *C* factor values from census crop totals and verbal descriptions of farming practices for the major crops grown in the Lake Simcoe–Couchiching Basin. Similarly, Busacca *et al.* (1993) calculated *C* and *P* factor values from farm records and interviews with landowners. Given the diversity of approaches that have been implemented for estimating these values, it is surprising how little attention has been paid to the sensitivity of model predictions to the source, resolution and accuracy of these factor values.

Additional problems are likely to occur because automated remote sensing classification methods are not able to distinguish the vegetation types of interest to soil conservationists. Most land managers are interested in Anderson level III vegetation categories at the species level (Anderson *et al.*, 1976) but automated classification accuracies for these classes are generally as low as 65–75 percent (Skidmore and Turner, 1988). This confusion arises because dissimilar vegetation types may have similar spectral signatures (Gates, 1980) and many crops and grasses have seasonally variable signatures that show rapid responses to varying precipitation amounts (Pickup *et al.*, 1994; Loveland *et al.*, 1995). Regardless of future improvements in remote sensing technology, such as imaging spectrometers (Thomas and Ustin, 1987), which produce a reflectance spectrum for each pixel in the image, there will always be some inherent confusion between spectral reflectance and vegetation type.

Two of the three applications also used the GIS to calculate slope gradients and slope lengths for a series of DEM grid cells. These values were then used with the USLE to estimate *LS* factor values (equation 6.2), but they could just as easily have been used with RUSLE (equations 5a, b) or the new slope steepness factor equation:

$$S = -1.5 + \frac{17}{1 + \exp(2.3 - 6.1 \sin \beta)} \tag{6.7}$$

where β is the slope angle in degrees (Nearing, 1997). This role seems straightforward given the presence of flow tracing (slope length) and slope gradient functions in most raster-based GIS; however, the choice of grid resolution of the DEM and the need to distinguish areas of net erosion and net deposition may lead to unexpected and undesirable results.

Hession and Shanholtz (1988), for example, used a 200 meter DEM and calculated average slope gradients from each center cell to its eight neighbors in a 3×3 cell

moving window. This average slope term does not match that used in the USLE and RUSLE models. James and Hewitt (1992), on the other hand, utilized a 90 meter DEM and calculated slope gradients following the path of steepest descent for the center cell in each 3×3 cell moving window. These slope gradients may not match those required by the model either. Hodgson (1995) showed that the methods used by Hession and Shanholtz (1988) and James and Hewitt (1992) produce slope gradients and aspects that are most closely associated with representative cell sizes approximately twice the initial DEM grid resolution. There are two potential problems. First, the USLE was not developed with slope gradients calculated over distances of 180–400 meters in mind. Second, numerous studies have suggested that DEM grid resolutions in the 2–20 meters range may be required for spatially distributed modeling in complex terrain (Moore *et al.*, 1993a; Zhang and Montgomery, 1994; Mitasova *et al.*, 1996). Fine-resolution DEM are required to represent the land surface (Gao, 1997) and generate slope lengths of similar magnitude to those that were used to develop the USLE and RUSLE models.

There are at least two other problems with the approaches adopted in these early applications. First, neither study mentioned the need to distinguish areas experiencing net erosion and net deposition before applying the model so that erosion may have been predicted in depositional as well as erosional areas. Second, the form of the USLE that was used in these applications probably meant that erosion was underestimated by approximately 33 percent (i.e., $1/(m+1)$ where $m = 0.5$) at each DEM grid location in the erosional areas. Moore and Wilson (1992) and Desmet and Govers (1996b) have both proposed GIS-based methods for estimating the *LS* factor that circumvent these problems; however, their methods introduce several new complications as discussed in the next section.

6.3.2 Exploiting GIS to develop new or improved models

At least three types of innovation have been proposed to circumvent some of the problems with the application of the USLE and RUSLE models to catchments and larger areas. The first set aims to provide improved estimates of one or more model inputs. The final pair provides opportunities to consider the effects of hydrology more directly in the soil erosion modeling environment, and is related to the extent to which their roots can be traced to the USLE.

The first set of innovations has utilized advances in measurement and/or interpolation techniques to generate improved estimates of one or more model inputs. Vieux and Farajalla (1996), for example, examined the potential of using the high resolution rainfall measurements gathered with Doppler radar by the US National Weather Service in distributed rainfall-runoff models. Burrough *et al.* (1997) reviewed the development of conceptual paradigms of soil classification and mapping over the past thirty years. The early models utilized crisp classes in attribute space linked to crisply delineated mapping units in geographical space. Most of the model inputs required by the USLE and RUSLE anticipate these types of data. The most recent models of soil classification and mapping have utilized fuzzy classification and geostatistical interpolation for simultaneously handling continuous variation in both attributes and location. Many of these applications have combined soil profile data with topographic attributes derived from DEM and satellite data inside GIS to generate spatially distributed predictions of one or more soil properties. Zhu (1997), for

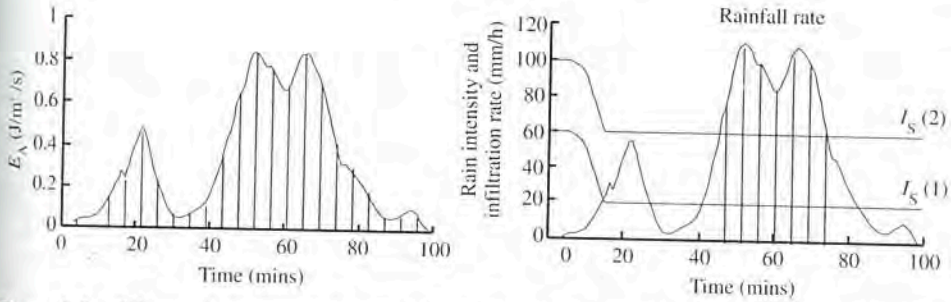

Figure 6.3 Schematic representation of EI_{30} index in relation to temporal variations in rainfall, kinetic energy flux E_A and rainfall intensity. The EI_{30} is twice the product of the shaded areas. Examples of temporal variations in soil infiltration rate $I_s(1)$ and $I_s(2)$ that might apply under these circumstances (see Figure 6.4) are also shown. (After Kinnell *et al.*, 1995, p. 1450.)

example, implemented one of these new fuzzy logic-based models in the Lubrecht Experimental Forest of western Montana, and showed that the information represented in this model has a higher resolution at both the attribute and spatial levels compared with the conventional soil map of the area. Other applications have used these concepts to improve the ways in which uncertainty and errors in model inputs and model predictions are handled (Bell *et al.*, 1994; Lark and Bolam, 1997). This shift from crisp to fuzzy classification and mapping paradigms has implications for the capture and display of other types of environmental information as well.

A second set of innovations has aimed to improve individual terms in the USLE and RUSLE models. Kinnell *et al.* (1995), for example, proposed a new rainfall-runoff factor, and Nearing (1997) proposed a new slope steepness factor (equation 6.7). The new rainfall-runoff factor assumes that soil loss is dependent on runoff (as in the USLE and RUSLE) but allows the 'bulk' sediment concentration (storm soil loss/storm runoff) for an event to vary with storm energy and the kinetic energy per unit quantity of rain (Kinnell, 1997). The product of storm rainfall kinetic energy (E in Figure 6.3) and the maximum rainfall intensity measured over 30 minutes (I_{30} in Figure 6.3) has been used as the R factor in the USLE throughout its history. This EI_{30} index does not consider variations in runoff rate that may result from differences in infiltration rates such as those indicated in Figure 6.3 and cause variations in erosion rates similar to those illustrated in Figure 6.4. Kinnell *et al.* (1995) examined erosion data from non-vegetated plots at Holly Springs, Missouri, and demonstrated that the $I_X E_A$ index is superior to the EI_{30} index because it accounts for the processes of detachment and transport better than the EI_{30} index. This $I_X E_A$ index, first proposed by Kinnell (1983), is based on the product of the excess rainfall rate I_X and the rate of expenditure of rain kinetic energy E_A. Rainfall kinetic energies are computed from:

$$E_A = 1099\, I\, [1 - 0.72 \exp(-1.27\, I)] \tag{6.8}$$

where E_A has units of foot-ton per acre per hour and I is rainfall intensity in inches per hour. This equation follows directly from the intensity-unit kinetic energy relationship used by Renard *et al.* (1993) in RUSLE (Kinnell *et al.*, 1995). The excess rainfall term I_X, which serves as a surrogate for the runoff rate Q, is the difference between the rainfall intensity and infiltration rate I_S.

This modified form of the USLE offers two major potential advantages. First, it provides a model that may be better suited to predicting event erosion. Hence, the

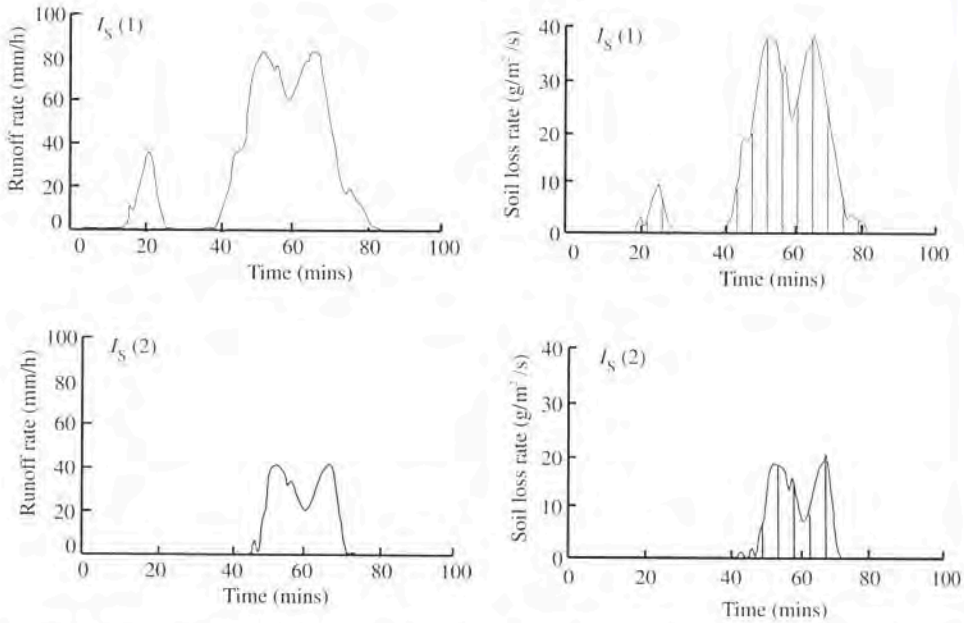

Figure 6.4 Possible variations in runoff and soil erosion resulting from rainfall infiltration conditions shown in Figure 6.3. (After Kinnell *et al.*, 1995, p. 1450.)

modified model produced a 15 percent improvement in the prediction of event erosion on non-vegetated field plots at Holly Springs (Kinnell, 1997). This level of improvement can be expected at sites at which rainfall energy has an appreciable impact on soil loss (i.e., non-vegetated field plots under natural rainfall) and, in general, the importance of this innovation will increase as the infiltration capacity of the soil increases. The second advantage of the modified model is that it provides a spatially distributed R factor when rainfall is uniform over a catchment. Spatially distributed annual or monthly average estimates of I_X (and therefore the $I_X E_A$ index) can be obtained from a GIS soil layer that includes infiltration rate as an attribute (Maidment, 1996; Wilson and Gallant, 1996).

These potential advantages are at least partially offset by the empirical basis of the original USLE model and the knowledge that runoff is implicitly considered in the other model inputs. This state of affairs means that all of the other factors (K, C, P, L and S) would need to be re-evaluated before this modified form of the USLE could be used in place of the original USLE or RUSLE models. Kinnell *et al.* (1995) generated new K factor values for 16 soils at Holly Springs, but their choice of non-vegetated plots avoided the need to develop new C and/or P factor values. Developing new factor values for a larger number of soils and crops would be an enormous undertaking notwithstanding the availability of the data that were used to develop the original USLE and RUSLE models.

The third and potentially most important set of innovations have tackled the slope gradient and slope length terms in the USLE and RUSLE. Moore and Wilson (1992) proposed a pair of simple erosion indices that account for the major hydrological and terrain factors affecting erosion, and implemented them in EROS (Wilson and Gallant, 1996). These indices incorporate a dimensionless sediment transport capacity that is a non-linear function of specific discharge and slope. They are derived from the

transport capacity limiting sediment flux in the Hairsine–Rose (Hairsine and Rose, 1991, 1992a, b), WEPP (Laflen *et al.*, 1991a, b) and catchment evolution (Willgoose *et al.*, 1991) erosion theories (Moore *et al.*, 1992). The first index calculates a spatially distributed sediment transport capacity and the second index distinguishes net erosion/deposition areas. Both indices can be easily extended to three-dimensional terrain, they can account for different runoff-producing mechanisms and soil properties using a spatially distributed weighting function, and they can be implemented in a GIS (Moore and Wilson, 1992, 1994).

The first index calculates the spatial distribution of soil loss potential with a simple dimensionless transport capacity index Tc that can be written as:

$$Tc_j = \left(\frac{\sum_{i \in C_j} \mu_i a_i / b_i}{22.13} \right)^m \left(\frac{\sin \beta_j}{0.0896} \right)^n \tag{6.9}$$

where μ_i is a weighting coefficient ($0 \leq \mu_i \leq 1$) that is dependent on the runoff generation mechanism and soil properties (i.e. infiltration rates), a_i is the area of the ith cell, b_i is the width of each cell, β_j is the slope in degrees, m and n are constants (0.6 and 1.3, respectively), and C_j is the set of i element indices which are hydrologically connected to cell j. When $\mu = 0$, no rainfall excess is generated; when $\mu = 1$, rainfall excess of 100 percent is generated.

The second index represents the change in sediment transport capacity across a grid cell ΔTc and provides a possible measure of the erosion or deposition potential in each cell (Moore and Burch, 1986a, b). The change in sediment transport capacity can be written as:

$$\Delta Tc_j = \varphi \left[\left(\sum_{i \in C_{j-}} \mu_i a_i / b_{j-} \right)^m (\sin \beta_{j-})^n - \left(\sum_{i \in C_j} \mu_i a_i / b_j \right)^m (\sin \beta_j)^n \right] \tag{6.10}$$

where φ is a constant, subscript j signifies the outlet of cell j, and $j-$ signifies the inlet to cell j, and C_j is the set of i element indices which are hydrologically connected to cell j minus the current cell (Moore *et al.*, 1992). Moore and Wilson (1992, 1994) hypothesized that a positive value of ΔTc_j indicates net deposition and a negative value indicates net erosion.

The number and source of input values used in equations (6.9) and (6.10) depend on the method used in EROS to estimate weighting coefficients. Three options are provided. The first option assumes that rainfall excess is generated uniformly over the entire catchment (i.e. $\mu_i = \mu = 1$). The second option assumes Hortonian overland flow in which μ_i is spatially variable and a function of the infiltration characteristics of the soil. The final option assumes saturation overland flow in which overland flow occurs only in zones of saturation in the landscape (Wilson and Gallant, 1996). Moore and Wilson (1992, 1994) calculated the slope gradient and specific catchment area terms in these equations with TAPES-G (Gallant and Wilson, 1996). This grid-based terrain analysis program calculates a variety of primary topographic attributes by applying a second-order, finite-difference scheme centered on the interior node of a moving 3×3 square-grid network similar to many raster-based GIS.

The uniform rainfall excess method uses the slope and drainage area terms with simplified versions of equations (6.8) and (6.9) as follows:

$$Tc_j = \left(\frac{As}{22.13} \right)^m \left(\frac{\sin \beta}{0.0896} \right)^n \tag{6.11}$$

$$\Delta Tc_j = \varphi\,[As_{j-}^{m}(\sin\beta_{j-})^{n} - As_j^{m}(\sin\beta_j)^{n}] \tag{6.12}$$

where φ is a constant, As is the specific catchment area or drainage area in meters squared per unit width in meters orthogonal to a flowline, and β is the slope in degrees. Mitasova *et al.* (1996) implemented continuous forms of these equations plus spline-based DEMs with tunable tension and smoothing and the vector-grid flow-routing method (described below) in the GRASS GIS. They argued that this approach increases the accuracy and reliability of topographic analysis, although more work is required to evaluate the benefits and costs of implementing these methods. Their model runs predicted erosion in areas with an increase in sediment transport capacity and deposition in areas with a decrease in sediment transport capacity. The net erosion areas coincided with areas of profile convexity and tangential concavity (flow acceleration and convergence), whereas the net deposition areas coincided with areas of profile concavity (decreasing flow velocity). These patterns matched those observed in a variety of field environments by Martz and DeJong (1987), Foster (1990), Sutherland (1991), and Busacca *et al.* (1993).

The Hortonian overland flow method (second option in equations 6.9 and 6.10) should be selected if runoff is to be determined by infiltration excess and one has a file containing multiple soil polygons with weighting factors. EROS reads this file and performs a series of point-in-polygon overlays to assign weighting factors to individual DEM grid points. Drainage areas are recalculated using these weights and one of the flow routing algorithms discussed below, and used with slope gradients to estimate Tc. This approach is conceptually similar to that proposed by Kinnell *et al.* (1995).

The saturation overland flow method (third option) should be selected if runoff is to be determined by surface saturation controlled by a user-specified critical wetness index. For this case, $\mu_j = 0$ when $\ln(As/\tan\beta) < W_c$, and $\mu_j = 1.0$ otherwise, where $\ln(As/\tan\beta)$ is a steady-state topographic wetness index (Moore *et al.*, 1988, 1993b) and W_c is a user-specified critical topographic wetness index that identifies the location of zones of surface saturation in the landscape. Moore *et al.* (1992) used a critical wetness index of 6.0 and found that $Tc > 2.5$ showed good agreement with areas of degradation observed in a 9.6 hectare watershed in Queensland, Australia during 1979–80 when vegetation was sparse.

Equations (6.9)–(6.12) can be implemented in raster-based GIS, although the quality of the output will vary with the choice of DEM, resolution, and flow routing algorithm. The resolution and vertical accuracy of available DEMs often cause problems because of insufficient vertical resolution and the presence of numerous pits that trap flow lines (Jenson and Domingue, 1988; Martz and Garbrecht, 1992; Mitasova *et al.*, 1996; Gao, 1997). In addition, many of the flow-routing algorithms implemented in raster-based GIS utilize a limited number of flow directions and produce unrealistic results. The choice of flow routing algorithm will affect the derivation of the specific catchment area and steady-state topographic wetness index terms used in equations (6.9) and (6.10) (Desmet and Govers, 1996a; Repetto and Wilson, 1999). There are at least six flow-routing algorithms that can be used in raster-based GIS and related software.

The *D8* (deterministic-eight node) single flow direction (sfd) algorithm developed by O'Callaghan and Mark (1984) allows flow from a node to only one of eight nearest neighbors based on the direction of steepest descent. This algorithm tends to produce flow in parallel lines along preferred directions, which will only agree with the aspect when aspect is a multiple of 45°, and it cannot model flow dispersion (Moore *et al.*,

1993a). The *D8* algorithm is used in ARC/INFO and remains the most commonly available method for determining drainage areas notwithstanding these limitations. The *Rho8* (random-eight node) sfd algorithm developed by Fairfield and Leymarie (1991) is a stochastic version of the *D8* algorithm in which the expected value of the direction is equal to the aspect. This algorithm cannot model flow dispersion (like the *D8* algorithm), but it does simulate more realistic flow networks. With this algorithm, long parallel flow paths are broken up at the cost of many more cells without upslope connection, distorting the distribution of contributing area.

The *FD8/FRho8* multiple flow direction (mfd) algorithms are modifications of *D8* and *Rho8* that allow flow dispersion or catchment spreading to be represented (Moore *et al.*, 1993a). This pair of algorithms allows flow to be distributed to multiple nearest-neighbor nodes in upland areas above defined channels and uses the *Rho8* or *D8* algorithms below points of channel initiation. The proportion of flow or upslope contributing area assigned to multiple downslope nearest neighbors above channels is determined on a slope-weighted basis using methods similar to those proposed by Freeman (1991) and Quinn *et al.* (1991). Holmgren (1994) and Quinn *et al.* (1995) proposed a new (fourth) method in which the mfd algorithm gradually changes to the sfd algorithm as the upslope contributing area increases. Both of these mfd algorithms tend to generate much more realistic, smoother distributions of upslope contributing area compared to the sfd algorithms (Quinn *et al.*, 1991; Wolock and McCabe, 1995; Moore, 1996).

The *DEMON* algorithm of Costa-Cabral and Burges (1994) generates flow in each source pixel and follows it down a stream tube until the edge of the DEM or a pit is encountered. These stream tubes expand and contract in response to the DEM surface and thus naturally model both convergence and divergence. Costa-Cabral and Burges found that the mfd algorithms discussed above generated errors under some conditions and that the *DEMON* algorithm shows the differences between convergent and divergent areas more accurately than both the sfd and mfd algorithms. The *D8*, *Rho8*, *FD8/FRho8*, and *DEMON* algorithms have all been implemented in TAPES-G (Gallant and Wilson, 1996).

The sixth and final algorithm uses a *vector-grid* approach and is implemented as the *r.flow* routine in the GRASS GIS (Mitasova and Hofierka, 1993; Mitasova *et al.*, 1995, 1996). Flow lines are constructed downhill from each grid cell until they reach a cell with a slope lower than some specified minimum, a boundary line, or some other barrier to calculate upslope contributing areas. These flow lines can follow 360 directions of flow and they are represented in a vector format. The points defining the flow lines are computed as the points of intersection of a line constructed in the flow direction given by the aspect angle and a grid cell edge. The *DEMON* and *vector-grid* algorithms share many similarities and are likely to produce similar results.

The results presented above and coincident advances in GIS technology may allow us to improve empirical models like the USLE and RUSLE and/or to replace them altogether with new erosion models in the next few years. The choice of flow-routing algorithm is important in both cases because the concept of specific catchment area is conceptually and physically a far superior surrogate for runoff and discharge than the slope length terms used by the USLE and RUSLE models (Moore and Wilson, 1992, 1994; Mitasova *et al.*, 1996).

Two innovations incorporating this concept have been proposed to improve the USLE and RUSLE models. First, Moore and Wilson (1992) have argued that *Tc* is equivalent to the length-slope factor in RUSLE for hillslopes with no convergence or

divergence. They used values of $m = 0.6$ and $n = 1.3$ in equation (6.11) and showed that this equation produced results consistent with equations (6.5a) and (6.5b) in RUSLE for slope lengths of less than 100 meters and slope angles of less than 14°. Second, Desmet and Govers (1996b) proposed the following equation to calculate the USLE and RUSLE *LS* factors over a two-dimensional landscape:

$$LS_{i,j} = \frac{S_{i,j}\,(As_{i,j-\mathrm{out}}^{m+1} - As_{i,j-\mathrm{in}}^{m+1})}{(As_{i,j-\mathrm{out}} - As_{i,j-\mathrm{in}})\,22.13^{m}} \tag{6.13}$$

where $LS_{i,j}$ is the topographic factor for a grid cell with coordinates i,j, $As_{i,j-\mathrm{out}}$ is the unit contributing area at the outlet of the grid cell with coordinates i,j in square meters per meter, $As_{i,j-\mathrm{in}}$ is the unit contributing area at the inlet of the grid cell with coordinates i,j in meters squared per meter, and m is the USLE or RUSLE length exponent. Their Fortran program reads and writes information in the same format as that used by the IDRISI GIS (Eastman, 1992). The slope length part of this method is conceptually similar to the approach of Foster and Wischmeier (1974) in that it treats each cell as a uniform slope segment and calculates the average soil loss for each slope segment. Both of these methods represent finite difference approximations of the point method shown in equation (6.6) (Mitasova *et al.*, 1997). However, Desmet and Govers (1996b, 1997) also used specific catchment area in place of slope length and argued that these changes make the USLE applicable to complex terrain.

There are at least three problems that argue against using equation (6.11) (Moore and Wilson, 1992) or equation (6.13) (Desmet and Govers, 1996b) in place of the RUSLE equations in a GIS:

1 The USLE and RUSLE models were developed for planar hillslopes that only occur on research plots and in farming systems using furrow irrigation. Figure 6.5 shows the spatial footprints for the RUSLE slope length and specific catchment area concepts on planar and convergent hillslopes. Moore and Wilson (1994) compared specific catchment area in square meters per meter and flowpath length in meters on a cell-by-cell basis in a small Montana cropland catchment, and found that 79 percent of the cells located above the channel system were located on divergent ($As/\lambda < 0.8$) or convergent ($1.2 < As/\lambda < 3.0$) hillslopes. Clearly, the paucity of planar slopes in natural landscapes may help to explain the large discrepancies often reported between predicted and observed erosion rates (for example, Busacca *et al.*, 1993).

2 The RUSLE equations were developed for detachment-limited erosion (on planar slopes) and the correlation noted above between the topographic factors for the transport-limited (equations 6.11 and 6.13) and detachment-limited (equations 6.5a and 6.5b) conditions occurs because both are functions of runoff and slope gradient (Foster, 1994; Mitasova *et al.*, 1997). Mitasova *et al.* (1997) used a series of field experiments to demonstrate that the approach captured in equation (6.13) neglects important physical processes and that the results of using it clearly contradict experimental data. Similarly, their comparison of the net deposition areas computed with terrain analysis methods and the net deposition areas derived from published soil maps by Desmet and Govers (1997) also highlights the problems that can occur when different data sources are combined in a GIS.

3 The empirical basis of the USLE and RUSLE models coupled with the knowledge that the effects of runoff are implicitly incorporated in several other terms means

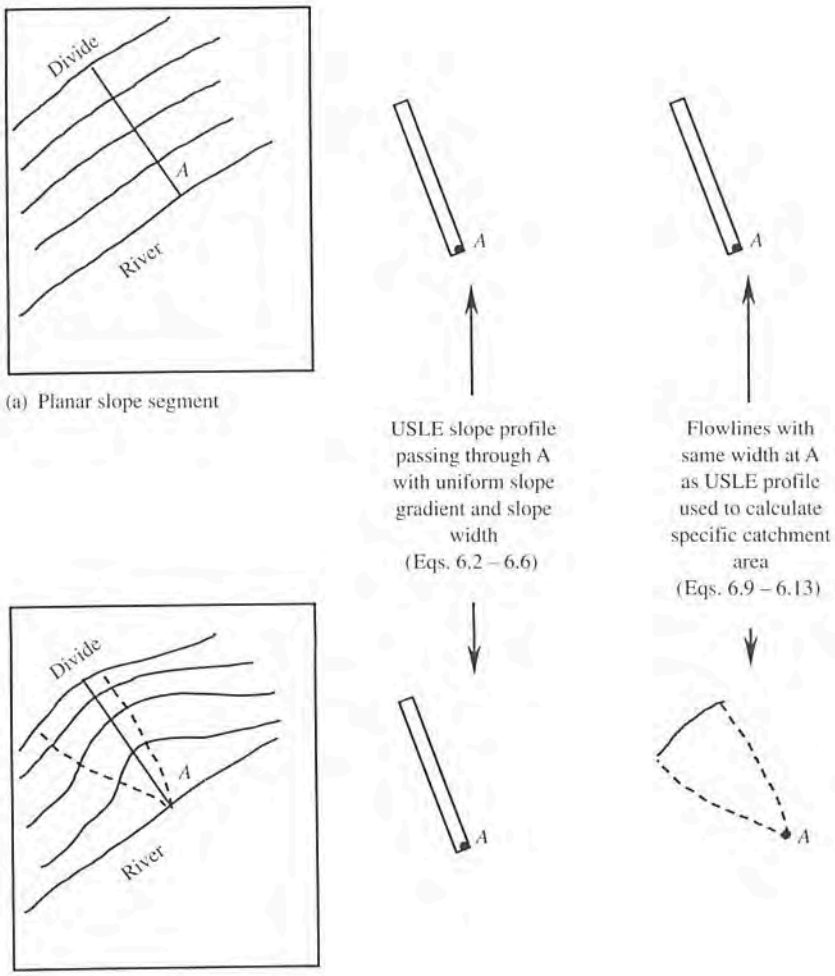

Figure 6.5 Schematic diagrams showing spatial footprints for USLE slope length and specific catchment area concepts on (a) planar and (b) convergent hillslopes.

that more direct consideration of slope convergence and divergence in the *LS* factor is likely to affect a number of other RUSLE factors as well (Foster, 1994; McCool, 1994).

The paucity of planar hillslopes in natural landscapes and failure to incorporate the effects of flow convergence and divergence highlight the shortcomings of the USLE and RUSLE models. This state of affairs favors using the concept of specific catchment area in conjunction with the new data products noted earlier as building blocks in a series of new GIS-based erosion models. One such model is briefly described below.

6.3.3 An exemplary GIS-based soil erosion model

Mitas *et al.* (1996) used the multivariate data processing, analysis and visualization tools available in the GRASS GIS (Mitasova *et al.*, 1995) to simulate the impact of complex terrain and various soil and land cover changes on the spatial distribution of soil erosion and deposition. Multivariate regularized splines with tension were used to represent the relevant data as continuous fields and a series of differential equations controlling the evolution of the key processes were used to predict the future states of these fields. Maidment (1996) and Kemp (1997a, b) provide extensive reviews of the basic features and likely consequences of using these data types and analytical methods for distributed environmental modeling.

Mitas *et al.* (1996) used Monte Carlo stochastic methods to solve the 2D continuity equation for steady-state overland flow, rewritten in the operator form, as:

$$W[h^{5/3}(r)] = -\frac{e}{2}\nabla^2[h^{5/3}(r)] + \nabla[h(r)v(r)] = i(r) \tag{6.14}$$

where W is the operator, h is the water depth in meters, $r = \{x,y\}$ is the position in meters, e is the diffusive constant, v is the flow velocity in meters per second, and i is the rainfall excess (rainfall minus infiltration) in meters per second. The velocity v is related to h via Mannings equation:

$$v = \frac{1}{n} R^{2/3} S^{1/2} \tag{6.15}$$

where n is a roughness coefficient related to flow resistance and R is the hydraulic radius of the channel. For overland flow, R can be approximated with water depth h (Haan *et al.*, 1994).

The sediment flux and erosion/deposition in complex terrain were estimated using the appropriate equations for continuity of mass (Foster and Meyer, 1972; Govindaraju and Kavvas, 1991) such that:

$$\begin{aligned}\text{Sources} - \text{Sinks} &= D_r(r,t) + D_i(r,t) \\ &= C[T(r,t) - |q_s(r,t)|] + D_i(r,t)\end{aligned} \tag{6.16}$$

where D_r is the rill detachment or deposition rate, D_i is the interrill contribution in kilograms per square meters per second, C is the first-order reaction coefficient dependent on soil and cover per meter, q_s is the sediment flux in kilograms per meter per second, and T is the sediment transport capacity in kilograms per meter per second given as:

$$T(r,t) = K_t[\tau(r,t) - \tau_{cr}(r,t)] \tag{6.17}$$

where K_t is the transport capacity coefficient, τ is the local shear stress, and τ_{cr} is the local critical shear stress (i.e. the shear stress necessary to mobilize particles). The sediment transport capacity T varies mainly as a function of the local shear stress given as:

$$\tau(r,t) = \rho_w g h(r,t) S(r) \tag{6.18}$$

where ρ_w is the mass density of water in kilograms per cubic meter, g is the gravitational acceleration constant in meters per second per second, and $S(r)$ is the slope. Under conditions of high velocity overland flow and easily erodible soil particles,

critical shear stress τ_{cr} becomes negligibly small relative to the available local shear stress τ. The rill detachment and deposition rate in equation (6.16) is proportional to the difference between transport capacity and sediment load (Foster and Meyer, 1972). This relationship is based on concepts of stream power (Haan *et al.*, 1994) and can be expressed as:

$$\frac{K_d}{D_c} + \frac{q_s}{T} = 1 \tag{6.19}$$

where K_d is the detachment capacity coefficient (rill erodibility) and D_c is the detachment capacity.

Mitas *et al.* (1996) were unable to implement the complete model because values for Manning's n, the detachment rate coefficient K_d and the sediment transport coefficient K_t are still under development for the large number and variety of soil and land cover conditions that occur in landscapes. They noted that the first-order reaction coefficient C, which is related to the detachment capacity and sediment transport capacity, is the most important factor controlling the spatial boundaries between erosion and deposition. In essence, the coefficients K_d, K_t, and C represent the balance between the ability of overland flow to transport material versus the ability to erode material as expressed in equations (6.16) and (6.19). The following simulations were used to illustrate the influence of uniform soil and cover parameters.

When the transport capacity coefficient K_t was held constant and the detachment capacity coefficient K_d was increased, C increased from 0.0005 to 100. Deposition occurred relatively high up the slope for values of $C > 1$ because the sediment flux quickly reached the sediment transport capacity. This is the transport-limited erosion/deposition case modeled by Moore and Wilson (1992) and Mitasova *et al.* (1996) and it is typical of sandy soils with relatively high fall velocities. In contrast, nearly all of the detached sediment will be carried to the stream for small values of C, which are likely to occur in clay soils with very low fall velocities and low detachment capacity. In both cases, the distribution of erosion and sedimentation across the landscape changed significantly while the magnitude of the sediment flux in the stream remained unchanged.

Changes in soil properties and land cover, which affect the sediment transport capacity, were investigated by varying the transport capacity coefficient K_t and holding the detachment capacity coefficient K_d constant. The magnitude of sediment delivered to streams and the spatial distribution of erosion/deposition were changed in this simulation. Hence, for $K_t \ll K_d$ and $C \gg 1$ most of the detached sediment was deposited before it reached the streams, and for $K_t \gg K_d$ and $C \ll 1$ there was minor deposition and most of the sediment was delivered to the stream network. This simulation and the previous one provide good examples of how calibrating an erosion model at a stream outlet may not account for major changes occurring across the modeled landscape.

The ratio between the transport capacity and erodibility is a function of soil and land-cover properties that are interrelated. To simulate this relationship, the transport capacity coefficient K_t and detachment capacity coefficient K_d were varied at the same rate so that the ratio C was constant. The magnitude of erosion but not the spatial distribution of erosion/deposition was changed in this simulation. This type of modeling effort can aid the analysis of erosion prediction techniques.

The spatial pattern of simulated erosion/deposition was predicted for homogeneous bare soil conditions and compared with the observed spatial distribution of colluvial

deposits for an experimental farm operated by the Technical University of Munich in Germany. The changes in the spatial pattern of erosion/deposition and sediment flux due to changes in rainfall and land cover were simulated over a one-year period for this same farm. The results from this simulation demonstrated that terrain controls the long-term spatial distribution of erosion and deposition. This seems reasonable because slope S controls the magnitude of local shear stress τ in equation (6.1). The results also demonstrated that land cover has a substantial impact on the magnitude of erosion.

The approach implemented by Mitas *et al.* (1996) incorporated at least three important innovations compared with previous applications. First, they used multivariate continuous fields in place of the discrete sets of points, lines, polygons and raster cells used in the earlier applications (see Maidment, 1996, and Kemp, 1997a, b for more complete discussions of these issues). Second, they used a steady-state 2D diffusive wave solution for the continuity equation to describe overland flow in contrast to most of the current GIS which only provide tools for the simplest approximate solution for steady-state flow and constant velocity based on upslope contributing area. The steady-state solutions utilized here are consistent, for example, with the latest soil erosion models implemented outside GIS (for example, WEPP; Flanagan and Nearing, 1995). Third, they presented the results in a series of animations that provided new opportunities to view spatially distributed results over timeframes ranging from individual storms to decades.

6.4 CONCLUSIONS

Soil erosion is a natural process that varies in space and time. Soil erosion rates are often accelerated by human land use. Soil erosion models need to consider soil detachment, transport and deposition to be applied to catchments and other large areas. The pervasive nature of these processes and widespread occurrence of soil erosion problems suggest a large and important role for GIS.

However, most of the soil erosion models in common use are empirical models that apply to a limited range of conditions. The USLE and RUSLE models, for example, apply only to those parts of the landscape in which erosion exceeds deposition and the rate of erosion is detachment-limited. Various improvements have been proposed to handle irregular slopes and to predict erosion at specific points in the landscapes without changing the basic properties of these models. Numerous GIS-based applications of these models during the past decade have failed to recognize these limitations and/or they have utilized GIS tools and data that were not compatible with those used for model development. This state of affairs demonstrates why GIS specialists need to invest considerable time and effort to understand the models they are using and why the results from many of the existing GIS-based model applications must be used with caution.

Fortunately, a second set of GIS-based applications has emerged during the past few years that clearly demonstrate the value of developing and implementing soil erosion models inside GIS. Moore and Wilson (1992, 1994), Mitasova *et al.* (1996), Mitas *et al.* (1996), Vieux and Farajalla (1996) and Zhu (1997), for example, show how GIS can be used to implement a series of physically based process descriptions and data representations to predict spatial and temporal patterns of soil erosion. The use of GIS to promote the progressive development of soil erosion models as documented

in this chapter illustrates the tremendous potential for using GIS to improve our understanding and representation of key environmental processes. The latest models incorporate detachment- and transport-limited erosion and deposition and may be able to predict the redistribution of sediment on hillslopes and the delivery of sediment to streams. This state of affairs represents a substantial advance over the earliest GIS-based modeling applications. However, further work is needed to develop spatially and temporally distributed parameter estimates for the large number and variety of soil and land cover conditions that occur in landscapes.

These results suggest that a series of models incorporating varying levels of complexity and input data will be required in the immediate future. Relatively simple, data-sparse models like those of Moore and Wilson (1992, 1994) could be used when the erosion problem is minor or data availability is poor. More complicated models with larger data demands like those of Mitas *et al.* (1996) could be used when the erosion problem is severe or data availability is good. Both types of model can be implemented in GIS so long as appropriate tools are available to prepare the input data and run the model(s). For example, the opportunities provided by fuzzy representations of attribute and spatial data for this type of modeling are enormous, and the choice of flow-routing algorithm is critical. GIS developers and users need to pay more attention to the model requirements (and model strengths and weaknesses) when developing and using these software tools and data models.

Acknowledgements

The work reported here was performed over a number of years and funded in part by grants to the first author from the Montana Agricultural Experiment Station and M.J. Murdock Charitable Trust. Contribution No. J-4015 of the Montana Agricultural Experiment Station. Ed DeYoung in the GIS Laboratory at the University of Southern California helped with the preparation of diagrams.

REFERENCES

ANDERSON, J.R., HARDY, E.E., ROACH, J.T. and WITMER, R.E., 1976. *A Land Use and Land Cover Classification System for Use with Remote Sensing*, United States Geological Survey Professional Paper No. 964, Washington, D.C.

BELL, J.C., CUNNINGHAM, R.L. and HAVENS, M.W., 1994. Soil drainage class probability mapping using a soil-landscape model. *Soil Science of America Journal*, **58**, 464–470.

BURROUGH, P.A., VAN GAANS, P.F.M. and HOOTSMANS, R., 1997. Continuous classification in soil survey: spatial correlation, confusion, and boundaries, *Geoderma*, **77**, 115–135.

BUSACCA, A.J., COOK, C. and MULLA, D.J., 1993. Comparing landscape-scale estimation of soil erosion in the Palouse using Cs-137 and RUSLE. *Journal of Soil and Water Conservation*, **48**, 361–367.

COSTA-CABRAL, M. and BURGES, S.J., 1994. Digital elevation model networks (DEMON): a model of flow over hillslopes for computation of contributing and dispersal areas. *Water Resources Research*, **30**, 1681–1692.

DESMET, P.J.J. and GOVERS, G., 1996a. Comparison of routing algorithms for digital elevation models and their implications for predicting ephemeral gullies. *International Journal of Geographical Information Systems*, **10**, 311–331.

DESMET, P.J.J. and GOVERS, G., 1996b. A GIS procedure for automatically calculating the USLE LS factor on topographically complex landscape units. *Journal of Soil and Water Conservation*, **51**, 427–443.

DESMET, P.J.J. and GOVERS, G., 1997. Comment on 'Modelling topographic potential for erosion and deposition using GIS', *International Journal of Geographical Information Systems*, **11**, 603–610.

EASTMAN, R.J., 1992. *IDRISI Users Guide (Version 4.0)*, Worchester, MA: Graduate School of Geography, Clark University.

FAIRFIELD, J. and LEYMARIE, P., 1991. Drainage networks from grid digital elevation models, *Water Resources Research*, **27**, 709–717.

FLACHE, W., AUERSWALD, K. and NEUFANG, L., 1990. Combining a modified USLE with a digital terrain model for computing high resolution maps of soil loss resulting from rain wash, *Catena*, **17**, 383–397.

FLANAGAN, D.C. and NEARING, M.A., 1995. *USDA Water Erosion Prediction Project (WEPP)*, National Soil Erosion Laboratory Report No. 10, United States Department of Agriculture, Agricultural Research Service, West Lafayette.

FOSTER, G.R., 1990. Process-based modeling of soil erosion by water on agricultural land, in Boardman, J.R., Foster, I.D.L. and Dearing, J.A. (eds) *Soil Erosion on Agricultural Land*, New York: Wiley, pp. 429–445.

FOSTER, G.R., 1991. Advances in wind and water prediction, *Journal of Soil and Water Conservation*, **46**, 27–29.

FOSTER, G.R., 1994. Comment on 'Length-slope factors for the Revised Universal Soil Loss Equation: simplified method of estimation', *Journal of Soil and Water Conservation*, **49**, 171–173.

FOSTER, G.R. and MEYER, L.D., 1972. A closed form erosion equation for upland areas, in Shen, H.W. (ed.) *Sedimentation: Symposium to Honor Professor H.A. Eistein*, Fort Collins, CO: Colorado State University, pp. 12.1–12.19.

FOSTER, G.R. and WISCHMEIER, W.H., 1974. Evaluating irregular slopes for soil loss prediction, *Transactions of the American Society of Agricultural Engineers*, **17**, 305–309.

FREEMAN, G.T., 1991. Calculating catchment area with divergent flow based on a regular grid, *Computers and Geosciences*, **17**, 413–422.

GALLANT, J.C. and WILSON, J.P., 1996. TAPES-G: A grid-based terrain analysis program for the environmental sciences, *Computers and Geosciences*, **22**, 713–722.

GAO, J., 1997. Resolution and accuracy of terrain representation by grid DEMs at a micro-scale, *International Journal of Geographical Information Science*, **11**, 199–212.

GATES, D.M., 1980. *Biophysical Ecology*, New York: Springer-Verlag.

GILLILAND, M.W. and BAXTER-POTTER, W., 1987. A geographic information system to predict non-point source pollution potential, *Water Resources Bulletin*, **23**, 281–291.

GLANZ, J., 1994. New soil erosion model erodes farmers' patience, *Science*, **264**, 1661–1662.

GOVINDARAJU, R.S. and KAVVAS, M.L., 1991. Modeling the erosion process over steep slopes: approximate analytical solutions, *Journal of Hydrology*, **127**, 279–305.

GRIFFIN, M.L., BEASLEY, D.B., FLETCHER, J.J. and FOSTER, G.R., 1988. Estimating soil loss on topographically non-uniform field and farm units, *Journal of Soil and Water Conservation*, **43**, 326–331.

HAAN, C.T., BARFIELD, B.J. and HAYNES, J.C., 1994. *Design Hydrology and Sedimentology for Small Catchments*, New York: Academic Press.

HAIRSINE, P.B. and ROSE, C.W., 1991. Rainfall detachment and deposition: sediment transport in the absence of flow-driven processes, *Soil Science Society of America Journal*, **55**, 320–324.

HAIRSINE, P.B. and ROSE, C.W., 1992a. Modelling water erosion due to overland flow using physical principles. I: Sheet flow, *Water Resources Research*, **28**, 237–243.

HAIRSINE, P.B. and ROSE C.W., 1992b. Modelling water erosion due to overland flow using physical principles. II: Rill flow, *Water Resources Research*, **28**, 245–250.

HESSION, W.C. and SHANHOLTZ, V.O., 1988. A geographic information system for targeting nonpoint-source agricultural pollution, *Journal of Soil and Water Conservation*, **43**, 264–266.

HODGSON, M.E., 1995. What cell size does the computed slope/aspect angle represent? *Photogrammetric Engineering and Remote Sensing*, **54**, 513–517.

HOLMGREN, P., 1994. Multiple flow direction algorithms for runoff modeling in grid-based elevation models: an empirical evaluation, *Hydrological Processes*, **8**, 327–334.

HUANG, S. -L. and FERNG, J. -J., 1990. Applied land classification for surface water quality management. II: Land process classification, *Journal of Environmental Management*, **31**, 127–141.

JAMES, D.E. and HEWITT, M.J., 1992. To save a river: building a resource decision support system for the Blackfoot River drainage, *GeoInfo Systems*, **2**, 36–49.

JENSON, S.K. and DOMINGUE, J.O., 1988. Extracting topographic structure from digital elevation model data for geographic information system analysis, *Photogrammetric Engineering and Remote Sensing*, **54**, 1593–1600.

KAUTZA, T.J., SCHERTZ, D.L., and WEESIES, G.A., 1995. Lessons learned in RUSLE technology transfer and implementation, *Journal of Soil and Water Conservation*, **50**, 490–493.

KEMP, K.K., 1997a. Fields as a framework for integrating GIS and environmental process models, Part 1, Representing spatial continuity, *Transactions in GIS*, **1**, 219–234.

KEMP, K.K., 1997b. Fields as a framework for integrating GIS and environmental process models, Part 2: Specifying field variables, *Transactions in GIS*, **1**, 235–246.

KINNELL, P.I.A., 1983. The effect of kinetic energy of excess rainfall on soil loss from non-vegetated plots, *Australian Journal of Soil Research*, **21**, 445–453.

KINNELL, P.I.A., 1997. Runoff ratio as a factor in the empirical modelling of soil erosion by individual rainstorms, *Australian Journal of Soil Research*, **35**, 1–13.

KINNELL, P.I.A., MCGREGOR, K.C. and ROSEWELL, C.J., 1995. The $I_X E_X$ index as an alternative to the EI_{30} erosivity index, *Transactions of the American Society of Agricultural Engineers*, **37**, 1449–1456.

LAFLEN, J.M., ELLIOT, W.J., SIMANTON, J.R., HOLZHEY, C.S. and KOHL, K.D., 1991a. WEPP: soil erodibility experiments for rangeland and cropland soils, *Journal of Soil and Water Conservation*, **46**, 39–44.

LAFLEN, J.M., LANE, L.J. and FOSTER, G.R., 1991b. WEPP: a new generation of erosion prediction technology, *Journal of Soil and Water Conservation*, **46**, 34–38.

LAFLEN, J.M., ELLIOT, W.J., FLANAGAN, D.C., MEYER, C.R. and NEARING, M.A., 1997. WEPP: predicting water erosion using a process-based model, *Journal of Soil and Water Conservation*, **52**, 96–102.

LARK, R.M. and BOLAM, H.C., 1997. Uncertainty in prediction and interpretation of spatially variable data on soils, *Geoderma*, **77**, 263–282.

LOVELAND, T.R., MERCHANT, J.W., BROWN, J.F., OHLEN, D.O., REED, B.C., OLSON, P. and HUTCHINSON, J., 1995. Seasonal land-cover regions of the United States, *Annals of the Association of American Geographers*, **85**, 339–355.

MAIDMENT, D.R., 1996. Environmental modeling within GIS, in Goodchild, M.F., Steyaert, L.T., Parks, B.O., Crane, M.P., Johnston, C.A., Maidment, D.R. and Glendinning, S. (eds) *GIS and Environmental Modeling: Progress and Research Issues*, Fort Collins, CO: GIS World Books, pp. 315–323.

MARTZ, L.W. and DEJONG, E., 1987. Using cesium-137 to assess the variability of net soil erosion and its association with topography in a Canadian prairie landscape, *Catena*, **14**, 439–451.

MARTZ, L. and GARBRECHT, J., 1992. Numerical definition of drainage network and subcatchment areas from digital elevation models, *Computers and Geosciences*, **18**, 747–762.

MCCOOL, D.K., 1994. Comments on Moore and Wilson, *Journal of Soil and Water Conservation*, **49**, 181.

MCCOOL, D.K., BROWN, L.C., FOSTER, G.R., MUTCHLER, C.K. and MEYER, L.D., 1987. Revised slope steepness factor for the Universal Soil Loss Equation, *Transactions of the American Society of Agricultural Engineers*, **30**, 1387–1396.

MCCOOL, D.K., FOSTER, G.R., MUTCHLER, C.K. and MEYER, L.D., 1989. Revised slope length

factor for the Universal Soil Loss Equation, *Transactions of the American Society of Agricultural Engineers*, **32**, 1571–1576.

MEYER, L.D., 1984. Evolution of the Universal Soil Loss Equation, *Journal of Soil and Water Conservation*, **39**, 99–104.

MITAS, L., MITASOVA, H., BROWN, W.M. and ASTLEY, M., 1996. Interacting fields approach for evolving spatial phenomena: application to erosion simulation for optimized land use, in NCGIA (ed.) *Proceedings of the Third International Conference Integrating GIS and Environmental Models, Santa Fe, NM, 21–25 January 1996*, Santa Barbara, CA: National Center for Geographic Information and Analysis, University of California (CD-ROM and WWW).

MITASOVA, H. and HOFIERKA, J., 1993. Interpolation by regularized spline with tension. II: Application to terrain modeling and surface geometry analysis, *Mathematical Geology*, **25**, 657–669.

MITASOVA, H., MITAS, L., BROWN, W.M., GERDES, D.P., KOSINOVSKY, I. and BAKER, T., 1995. Modeling spatially and temporally distributed phenomena: new methods and tools for GRASS GIS, *International Journal of Geographical Information Systems*, **9**, 433–456.

MITASOVA, H., HOFIERKA, J., ZLOCHA, M. and IVERSON, L.R., 1996. Modelling topographic potential for erosion and deposition using GIS, *International Journal of Geographical Information Systems*, **10**, 629–641.

MITASOVA, H., HOFIERKA, J., ZLOCHA, M. and IVERSON, L.R., 1997. Reply to Comment by Desmet and Govers, *International Journal of Geographical Information Systems*, **11**, 611–618.

MOORE, I.D., 1996. Hydrologic modeling and GIS, in Goodchild, M.F., Steyaert, L.T., Parks, B.O., Crane, M.P., Johnston, C.A., Maidment, D.R. and Glendinning, S. (eds) *GIS and Environmental Modeling: Progress and Research Issues*, Fort Collins, CO: GIS World Books, pp. 143–148.

MOORE, I.D. and BURCH, G.J., 1986a. Physical basis of the length-slope factor in the Universal Soil Loss Equation, *Soil Science Society of America Journal*, **50**, 1294–1298.

MOORE, I.D. and BURCH, G.J., 1986b. Modelling erosion and deposition: topographic effects, *Transactions of the American Society of Agricultural Engineers*, **29**, 1624–1630, 1640.

MOORE, I.D. and WILSON, J.P., 1992. Length-slope factors for the Revised Universal Soil Loss Equation: simplified method of estimation, *Journal of Soil and Water Conservation*, **47**, 423–428.

MOORE, I.D. and WILSON, J.P., 1994. Reply to 'Comment on "Length-slope factors for the Revised Universal Soil Loss Equation: simplified method of estimation" by George R. Foster', *Journal of Soil and Water Conservation*, **49**, 174–180.

MOORE, I.D., BURCH, G.J. and MACKENZIE, D.H., 1988. Topographic effects on the distribution of surface soil water and the location of ephemeral gullies, *Transactions of the American Society of Agricultural Engineers*, **31**, 1098–1107.

MOORE, I.D., WILSON, J.P. and CIESIOLKA, C.A., 1992. Soil erosion prediction and GIS: linking theory and practice, in Luk, S.H. and Whitney, J. (eds) *Proceedings of the International Conference on the Application of Geographic Information Systems to Soil Erosion Management*, Toronto: University of Toronto Press, pp. 31–48.

MOORE, I.D., LEWIS, A. and GALLANT, J.C., 1993a. Terrain attributes: estimation methods and scale effects, in Jakeman, A.J., Beck, M.B. and McAleer, M. (eds) *Modeling Change in Environmental Systems*, New York: Wiley.

MOORE, I.D., TURNER, A.K., WILSON, J.P., JENSON, S.K. and BAND, L.E., 1993b. GIS and land surface–subsurface process modeling, in Goodchild, M.F., Parks, B.O. and Steyaert, L.T. (eds) *Environmental Modeling with GIS*, New York: Oxford University Press, pp. 196–230.

MORGAN, K.M. and NALEPA, R., 1982. Application of aerial photographic and computer analysis to the USLE for areawide erosion studies, *Journal of Soil and Water Conservation*, **37**, 347–350.

MORGAN, K.M., LEE, G.B., KIEFER, R.W. and DANIEL, T.C., 1978. Prediction of soil loss on cropland with remote sensing, *Journal of Soil and Water Conservation*, **33**, 291–293.

MORGAN, K.M., MORRIS-JONES, D.R., LEE, G.B. and KIEFER, R.W., 1979. Cropping management using color and CIR aerial photographs, *Photogrammetric Engineering and Remote Sensing*, **45**, 769–774.

MORGAN, K.M., MORRIS-JONES, D.R. and LEE, G.B., 1980. Aerial photography as an aid to cropland erosion analysis, *Transactions of the American Society of Agricultural Engineers*, **23**, 907–913.

NEARING, M.A., 1997. A single, continuous function for slope steepness influence on soil loss, *Soil Science Society of America Journal*, **61**, 917–919.

NYERGES, T.L., 1992. Coupling GIS and spatial analytic models, in Bresnahan, P., Corwin, E. and Cowan, D.J. (eds) *Proceedings of the Fifth International Symposium on Spatial Data Handling*, Columbia, SC: University of South Carolina, pp. 534–542.

O'CALLAGHAN, J.F. and MARK, D.M., 1984. The extraction of drainage networks from digital elevation data, *Computer Vision, Graphics and Image Processing*, **28**, 323–344.

PICKUP, G., BASTIN, G.N. and CHEWINGS, V.H., 1994. Remote sensing-based condition assessment for non-equilibrium rangelands under large-scale commercial grazing, *Ecological Applications*, **4**, 497–517.

PIMENTAL, D., HARVEY, C., RESOSUDARMO, P., SINCLAIR, K., KURZ, D., MCNAIR, M., CRIST, S., SHPRITZ, L., FITTON, R., SAFFOURI, R. and BLAIR, R., 1995. Environmental and economic costs of soil erosion and conservation benefits, *Science*, **267**, 1117–1122.

QUINN, P.F., BEVEN, K.J., CHEVALLIER, P. and PLANCHON, O., 1991. The prediction of hillslope flow paths for distributed hydrological modeling using digital terrain models, *Hydrological Processes*, **5**, 59–79.

QUINN, P.F., BEVEN, K.J. and LAMB, R., 1995. The ln (a / tan β) index: how to calculate it and how to use it within the TOPMODEL framework, *Hydrological Processes*, **9**, 161–182.

RENARD, K.G., FOSTER, G.R., WEESIES, G.A. and PORTER, J.P., 1991. RUSLE: Revised Universal Soil Loss Equation, *Journal of Soil and Water Conservation*, **41**, 30–33.

RENARD, K.G., FOSTER, G.R., WEESIES, G.A., MCCOOL, D.K. and YODER, D.C., 1993. *Predicting Soil Erosion by Water: A Guide to Conservation Planning with the Revised Universal Soil Loss Equation (RUSLE)*, Handbook No. 703, Washington DC: United States Department of Agriculture.

RENARD, K.G., FOSTER, G.R., YODER, D.C. and MCCOOL, D.K., 1994. RUSLE revisited: status, questions, answers, and the future, *Journal of Soil and Water Conservation*, **49**, 213–220.

REPETTO, P.L. and WILSON, J.P., 1999. Effect of data source, grid resolution, and flow routing method on computed topographic attributes, in Wilson, J.P. and Gallant, J.C. (eds) *Hydrological, Geomorphological and Biological Applications of Digital Terrain Analysis*, New York: Wiley (in press).

RITCHIE, J.C. and MCHENRY, J.R., 1990. Application of radioactive fallout Cesium-137 for measuring soil erosion and sediment accumulation rates and patterns: A review, *Journal of Environmental Quality*, **19**, 215–233.

SIVERTUN, A., REINELT, L.E. and CASTENSSON, R., 1988. A GIS method to aid in non-point source critical area analysis, *International Journal of Geographical Information Systems*, **2**, 365–378.

SKIDMORE, A.K. and TURNER, B.J., 1988. Forest mapping accuracies are improved using a supervised non-parametric classifier with SPOT data, *Photogrammetric Engineering and Remote Sensing*, **54**, 1415–1421.

STEPHENS, P.R., MACMILLAN, J.H., DAIGLE, J.L. and CIHLAR, J., 1985. Estimating universal soil loss equation factor values with aerial photography, *Journal of Soil and Water Conservation*, **40**, 293–296.

SUTHERLAND, R.A., 1991. Caesium-137 and sediment budgeting within a partially closed drainage basin, *Zeitschrift für Geomorphologie*, **35**, 47–63.

THOMAS, R.W. and USTIN, S.L., 1987. Discriminating semi-arid vegetation using airborne imaging spectrometer data: a preliminary assessment, *Remote Sensing of Environment*, **23**, 273–290.

TIM, U.S., MOSTAGHIMI, S. and SHANHOLTZ, V.O., 1992. Identification of critical non-point source areas using geographic information systems and water quality modeling. *Water Resources Bulletin*, **28**, 877–887.

TOMLIN, C.D., 1980. *The Map Analysis Package*, New Haven, CT: School of Forestry and Environmental Science, Yale University.

VENTURA, S.J., CHRISMAN, N.R., CONNERS, K., GURDA, R.F. and MARTIN, R.W., 1988. A land information system for soil erosion control planning. *Journal of Soil and Water Conservation*, **43**, 230–233.

VIEUX, B.E. and FARAJALLA, N.S., 1996. Temporal and spatial aggregation of NEXRAD rainfall estimates on distributed storm runoff simulation, in NCGIA (ed.) *Proceedings of the Third International Conference Integrating GIS and Environmental Models, Santa Fe, NM, 21–25 January 1996*, Santa Barbara: CA, National Center for Geographic Information and Analysis, University of California (CD-ROM and WWW).

WARREN, S.D., DIERSING, V.E., THOMPSON, P.J. and GORAN, W.D., 1989. An erosion-based land classification system for military installations. *Environmental Management*, **13**, 251–257.

WILLGOOSE, G., BRAS, R.L. and RODRIGUEZ-ITURBE, I., 1991. A coupled channel network growth and hillslope evolution model. I: Theory. *Water Resources Research*, **27**, 1671–1684.

WILLIAMS, J.R. and BERNDT, H.D., 1972. Sediment yield computed with universal equation. *Journal of the Hydraulics Division, American Society of Civil Engineers*, **98**, 2087–2098.

WILLIAMS, J.R. and BERNDT, H.D., 1977. Determining the universal soil loss equation's length-slope factor for watersheds, in Foster, G.R. (ed.) *Soil Erosion: Prediction and Control*, Ankeny, IA: Soil Conservation Society of America, pp. 217–225.

WILSON, J.P., 1986. Estimating the topographic factor in the universal soil loss equation for watersheds. *Journal of Soil and Water Conservation*, **41**, 179–184.

WILSON, J.P., 1989. Soil erosion from agricultural land in the Lake Simcoe–Couchiching Basin 1800–1981. *Canadian Journal of Soil Science*, **69**, 137–151.

WILSON, J.P. and GALLANT, J.C., 1996. EROS: A grid-based program for estimating spatially-distributed erosion indices. *Computers and Geosciences*, **22**, 707–712.

WILSON, J.P. and RYAN, C.M., 1988. Landscape change in the Lake Simcoe–Couchiching Basin 1800–1983. *Canadian Geographer*, **32**, 206–222.

WISCHMEIER, W.H., 1976. Use and misuse of the univeral soil loss equation. *Journal of the Soil and Water Conservation*, **31**, 5–9.

WISCHMEIER, W.H. and SMITH, D.D., 1965. *Predicting Rainfall-erosion Losses from Cropland East of the Rocky Mountains*, Handbook No. 282, Washington DC: United States Department of Agriculture.

WISCHMEIER, W.H. and SMITH, D.D., 1978. *Predicting Rainfall Erosion Losses: A Guide to Conservation Planning*, Handbook No. 537, Washington DC: United States Department of Agriculture.

WOLOCK, D.M. and MCCABE, G.J., 1995. Comparison of single and multiple flow direction algorithms for computing topographic parameters in TOPMODEL. *Water Resources Research*, **31**, 1315–1324.

WOODWELL, G.M., HOBBIE, J.E., HOUGHTON, R.A., MELILLO, J.M., MOORE, B., PARK, A.B., PETERSON, B.J. and SHAVER, G.R., 1984. Measurement of changes in the vegetation of the earth by satellite imagery, in Woodwell, G.M. (ed.) *The Role of Terrestrial Vegetation in the Global Carbon Cycle: Measurement by Remote Sensing*, New York: Wiley, pp. 345–364.

YODER, D. and LOWN, J., 1995. The future of RUSLE: inside the new Revised Universal Soil Loss Equation. *Journal of Soil and Water Conservation*, **50**, 484–489.

ZHANG, W. and MONTGOMERY, D.R., 1994. Digital elevation model grid size, landscape representation and hydrologic simulations. *Water Resources Research*, **30**, 1019–1028.

ZHU, A.-X., 1997. A similarity model for representing soil spatial information. *Geoderma*, **77**, 217–242.